Spring 5-1-2023

Investigating the Phenotypic Effects of RING1- and YY1-Binding Protein (RYBP) in Glioblastoma Multiforme

Ronald W. Bucher
Winthrop University, rbucher@g.clemson.edu

May 2023

To the Dean of the Graduate School:

We are submitting a thesis written by Ronald William Bucher entitled “Investigating the Phenotypic Effects of RING1- and YY1-Binding Protein (RYBP) in Glioblastoma Multiforme.” We recommend acceptance in partial fulfillment of the requirements for the degree of Master of Science in Biology.

Daniel B. Stovall, Ph.D., Thesis Advisor

Victoria J. Frost, Ph.D., Committee Member

Kathryn P. Kohl, Ph.D., Committee Member

Matthew M. Stern, Committee Member

Takita Sumter, Ph.D., Dean, College of Arts and Sciences

Jack DeRochi, Ph.D., Dean, Graduate School

INVESTIGATING THE PHENOTYPIC EFFECTS OF RING1- AND YY1-BINDING PROTEIN (RYBP) IN GLIOBLASTOMA MULTIFORME

A Thesis

Presented to the Faculty

Of the

College of Arts and Sciences

In Partial Fulfillment

Of the

Requirements for the Degree

Of

Master of Science

In Biology

Winthrop University

May, 2023

By

Ronald William Bucher

Abstract

Glioblastoma multiforme (GBM) is an aggressive form of brain cancer that has horrendous survival outcomes with the use of current therapies. Further study into its molecular mechanisms will inform development of new, more effective treatments. The Polycomb protein RING1- and YY1- Binding Protein (RYBP) has emerged as an important gene in multiple cancers. In complex with other Polycomb proteins, RYBP acts to repress regions of chromatin, though it also performs other functions independent of these complexes. RYBP has a tumor suppressive role in various cancers, but may act as an oncogene in others, demonstrating its context-specific effects. The role of RYBP in GBM has not yet been elucidated. In GBM, RYBP expression is frequently downregulated compared to normal brain tissue, suggesting it may act as a tumor suppressor in GBM. Thus, we hypothesized that forced expression of RYBP in GBM cell lines would activate apoptosis while decreasing cell invasion, migration, and proliferation. We transduced U-118 or T98G GBM cell lines with lentivirus expressing RYBP or a GFP control and established stable cell lines. RYBP-expressing U-118 and T98G cells showed decreased migration in wound-healing assays and invasion in Matrigel-coated Boyden chamber assays when compared to control cells. SDS-PAGE and Western blots were performed to measure changes in epithelial-to-mesenchymal transition (EMT) and apoptotic protein markers among transduced cells, and WST-1 assays were conducted to study the changes in proliferation. Overall, our findings suggest RYBP exerts anti-tumor effects in GBM and acts as a tumor suppressor gene. Future work should investigate the mechanism of RYBP's phenotypic effects in GBM.

Table of Contents

List of Illustrations

Chapter One

Literature Review

Introduction

Cancer, a group of diseases that are defined by abnormal cells growing uncontrollably with the potential to invade other parts of the body, is the second leading cause of death worldwide, with almost 10 million deaths attributable in 2020 (Sung et al. 2021). Glioblastoma multiforme (GBM) is the most common malignant cancer of the central nervous system and originates from glial cells (Ostram et al. 2021). GBM can be differentiated into primary and secondary types based on cellular origin and genetic/epigenetic profiles, most notably through mutations in the isocitrate dehydrogenase 1 (*IDH1*) gene, which can be used as a diagnostic marker (Ohgaki and Kleihues 2013). Primary GBM typically arises quickly, directly from glial cells with very few cases displaying mutations in *IDH1*. Secondary GBM frequently has mutations in *IDH1* and displays signs of a precursor lesion that develops from lower grade astrocytomas. Primary GBM is usually observed in older patients and has a worse prognosis, while secondary GBM is more often found in children and has a better estimated outcome (Ohgaki and Kleihues 2013). Current treatments include chemotherapy, radiation, and surgery if possible. However, the prognosis for GBM is still horrendous. According to the *Central Brain Tumor Registry of the United States (CBTRUS) Statistical Report: Primary Brain and Other Central Nervous System Tumors Diagnosed in the United States in 2014-2018*, GBM patients have a median survival time of eight months and an estimated five-year survival rate of 7% regardless of treatment (Ostram et al. 2021).

Current treatments fail to improve survival due to their inability to completely eradicate the cancerous cell population, especially given the sensitive nature of the brain. Surgery, the primary method of treatment, is not always an option due to the particular location of the tumor and the extent to which it has integrated with the surrounding brain tissue (Fernandes et al. 2017). Further, brain surgery is extremely involved and poses many problems and complications not associated with other cancer types. Surgical

resection is often incomplete, so it is typically followed with radiation and chemotherapy treatments (Matthews et al. 2022). Radiation has proved to damage surrounding healthy tissue and lead to cognitive impairment as a result (Haldbo-Classen et al. 2021; Matthews et al. 2022). For this reason, radiation treatment must be balanced between eradicating the cancer and not doing too much surrounding tissue damage, which limits its efficacy. Chemotherapy can prove beneficial in combination with radiation, but getting the drug past the blood-brain barrier can prove challenging. Following initial treatment, resistance to chemotherapy often occurs, making future treatment difficult (Sun et al. 2022). New treatments, including targeted drug therapies and clinical trials, hold promise, but still have to be used in combination with chemotherapy and radiation (Fernandes et al. 2017). These fundamental shortcomings and the difficulty of treatment highlight the importance of developing new, increasingly targeted therapies. This will require an in-depth study of the molecular mechanisms that drive GBM progression to develop more effective treatment options.

RING1- and YY1- Binding Protein (RYBP, also known as DEDAF, YEAF1, AAP1, or APAP-1) is an evolutionarily conserved protein that plays important roles in human development and disease. RYBP was first characterized by Garcia et al. (1999) as an interacting partner of the mouse Polycomb group (PcG) proteins Yin Yang 1 (YY1), RING Finger Protein 1A (Ring1A), and RING Finger Protein 1B (Ring1B). Since then, RYBP's interactions with many other proteins have been characterized. In humans, the *RYBP* gene is located in sub-band 3 of band 1 on the short arm of the third chromosome (3p13) on the reverse strand. The initial RNA transcript of *RYBP* consists of four exons and three introns (Zheng et al. 2001). RYBP is a relatively short protein of 228 amino acids and is typically localized to the nucleus. Its nuclear localization signal is between Pro73 and Glu82 (Neira et al. 2021), although it has important apoptotic functions in the cytoplasm (Zheng et al. 2001; Tan et al. 2017). RYBP is thought to have relatively little native

secondary or tertiary structure but may adopt new conformations through binding DNA or proteins (Neira et al. 2009). The N-terminus has been seen to contain a DNA-binding Zinc Finger domain (position 25-52) (Garcia et al. 1999) while the C-terminus contains a binding domain for GABPB1 (position 143-226) (Sawa et al. 2002) and FANK1 (Ma et al. 2016). Meanwhile, the protein is decorated with various post-translational modifications along its length, such as phosphorylation and ubiquitination sites.

Little is currently understood about the molecular role of RYBP in GBM other than that it is frequently downregulated and associated with worse prognosis (Li et al. 2013). The fact that almost half of GBM patient samples have decreased RYBP expression relative to normal brain tissue suggests RYBP has a tumor suppressive role in GBM. Thus, we predicted that forced RYBP expression may yield increased apoptosis and decreased proliferation, migration, and invasion in GBM cell lines.

RYBP is a Polycomb Protein

One common driver of cancer, especially GBM, is epigenetic dysregulation. Polycomb group (PcG) proteins are important epigenetic regulators (Gao et al. 2012). First identified in *Drosophila melanogaster* as regulators of *Hox* gene expression (Lewis 1978), PcG proteins are now known to participate in functions such as stem cell differentiation, cancer epigenetics, and X chromosome-inactivation (recently reviewed in Geng and Gao 2020). PcG proteins are phylogenetically conserved chromatin modifiers that lead to transcriptional silencing (Gao et al. 2012) and exist as part of two main complexes: Polycomb repressive complex 1 and 2 (PRC1 and PRC2, respectively) (Paro 1990). These two complexes are responsible for histone tail modifications that lead to chromatin compaction and gene repression (Rose et al. 2016). The specific proteins constituting these complexes vary, creating subvariants of both PRC1 and PRC2. PRC2 contains a histone H3 lysine 27 (H3K27) methyltransferase that methylates H3K27 (H3K27me).

Canonical PRC1 is distinguished by the inclusion of chromobox (CBX) proteins. CBX, through its chromodomain, binds H3K27me to recruit other catalytic components of PRC1, like RING1. The recruitment and activity of PRC2 and canonical PRC1 are thus linked to jointly repress genomic regions, with canonical PRC1 recruited by PRC2-mediated H3K27me marks (Cao et al. 2002; Kuzmichev et al. 2002). Canonical PRC1's repressive action is seen to act most at the chromosome compaction level (Fursova et al. 2019). On the other hand, non-canonical PRC1s (ncPRC1) do not require H3K27me for their recruitment and binding to DNA. Rather, in ncPRC1, either RYBP or YAF2 proteins exclude the CBX subunit through competitive binding with RING1 (Gao et al. 2012). RYBP also has a DNA binding domain, thereby providing a mechanism where H3K27me, while important for canonical PRC1 recruitment, is not a necessary prelude for ncPRC1. NcPRC1 then acts as an E3 ubiquitin ligase, adding a single ubiquitin molecule to histone H2A at lysine 119 (H2AK119ub), which may in turn recruit PRC2 (Cao et al. 2005). Zhao et al. (2020) found that the RYBP-containing PRC1 complexes are crucial for inheritance of H2AK119ub on daughter DNA strands through a positive-feedback loop. RYBP binds existing H2AK119ub to recruit ncPRC1 to propagate H2AK119ub marks to surrounding nucleosomes in a histone H1-dependent manner (Arrigoni et al. 2006; Zhao et al. 2020). These results indicate the importance of ncPRC1 in maintenance and inheritance of gene repression and provide a mechanism by which ncPRC1 can recruit PRC2 as well as more ncPRC1 through a positive feedback loop. Thus, in the most recent model of PRC-mediated chromatin repression, ncPRC1 initiates gene repression and instigates H2A119ub marks that recruit PRC2, which in turn recruits canonical PRC1 via H3K27me. PRC1 then compacts chromatin in the surrounding area and maintains gene silencing, providing a mechanism by which Polycomb-compacted chromatin regions are formed (Fursova et al. 2019; Tamburri et al. 2020) (Figure 1). In support, the absence of ncPRC1 led to a full decompression of its target genes, denoting its significance in initiating gene

repression (Fursova et al. 2019). Conversely, RYBP in ncPRC1 also has a role in phase separation and orchestrating interactions between actively used portions of the chromosomes (Wei et al. 2022), demonstrating its wide range of actions in regulation.

When RYBP is absent, neural embryonic stem cells showed aberrant expression of neural marker genes such as *Pax6* and a reduction in matured neural cells (Kovacs et al. 2016). Sutus et al. (2022) demonstrated that embryonic stem cells not expressing RYBP used in *in vitro* neural cultures showed less differentiation, increased number of progenitor cells versus matured cells, and higher levels of *Pax6*. This reduced neural differentiation was attributed to increased retinoic acid signaling pathway activity due to loss of RYBP, which increased *Pax6* expression and lessened differentiation. RYBP further exhibited the ability to repress *Pax6* expression through ncPRC1, suggesting its importance in neural development (Sutus et al. 2022).

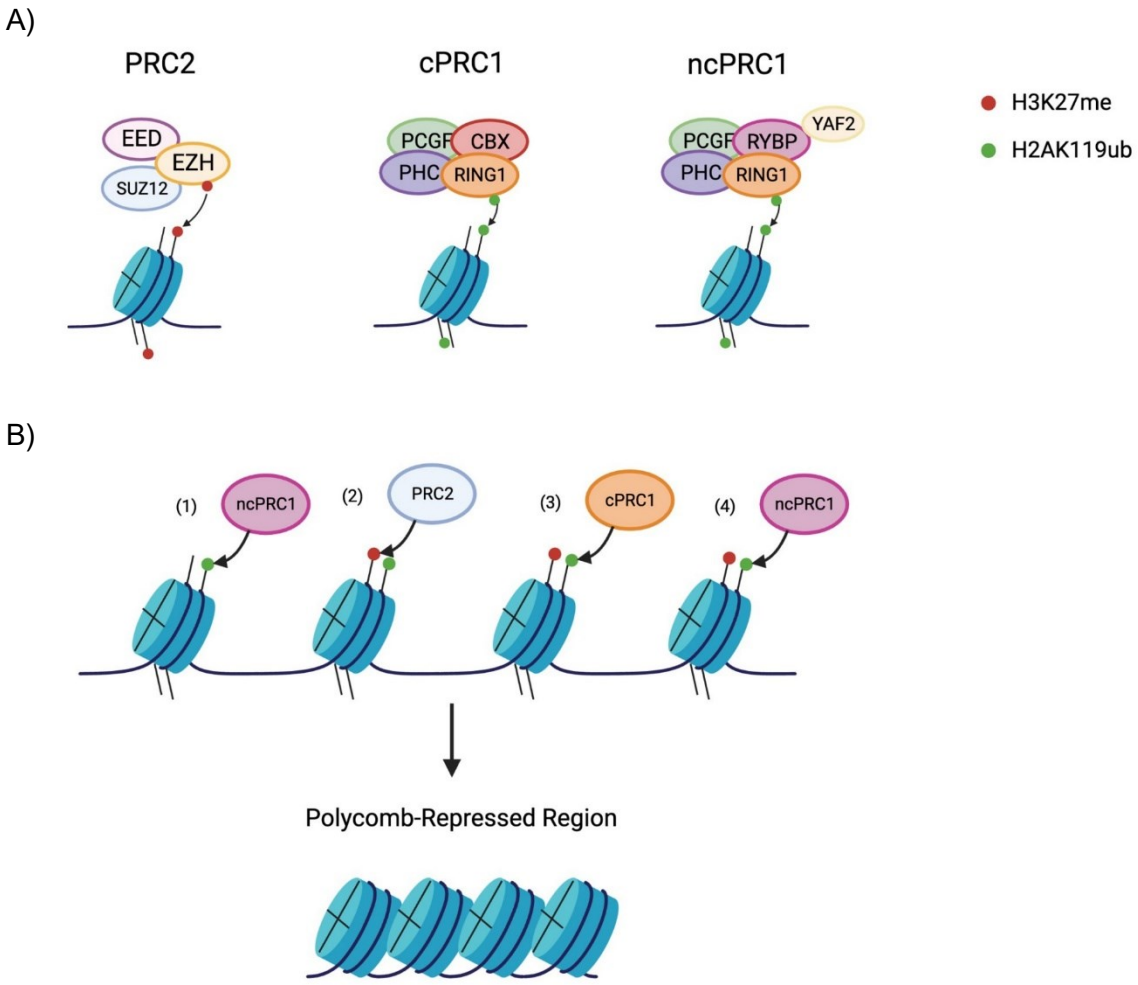

Figure 1. PRC Mediated Chromatin Compaction. A) The various components of PRC2, cPRC1, and ncPRC1. NcPRC1 is distinguished by the inclusion of RYBP/YAF2 subunits instead of the CBX subunit. PRC2 mediates H3K27me and both cPRC1 and ncPRC1 ubiquitinate H2AK119 (Created with BioRender.com, adapted from Chan and Morey 2019). **B)** The mechanism by which PRC mediated chromatin compaction occurs. NcPRC1 ubiquitinates H2AK119, in turn recruiting PRC2 to methylate H3K27(2). H3K27me serves as a recruiting factor for cPRC1 (3) or ncPRC1 (4) to further ubiquitinate surrounding histones leading to PRC-repressed chromatin regions (Created with BioRender.com, adapted from Bracken et al. 2019)

Another mechanism of RYBP regulation in ncPRC1 is through its interactions with ubiquitin protein ligase E3A (UBE3A) and RING1B. Li et al. (2019) found that RYBP leads to target gene repression through its multiple interactions with RING1B and UBE3A and subsequent activity on H2AK119ub. UBE3A is responsible for ubiquitinating RING1B to facilitate its degradation. RYBP can stop this ubiquitination by directly binding with RING1B, blocking UBE3A binding and activity. RYBP also can bind UBE3A prior to its binding of RING1B, leading to UBE3A ubiquitination and degradation. Finally, RYBP can bind with the RING1B/UBE3A complex to stop UBE3A's ubiquitination of RING1B. All of these mechanisms lead to increased RING1B stability, thereby increasing its repressive activity on its target genes through ncPRC1 (Li et al. 2019).

RYBP in ncPRC1 also has a role in DNA damage response (DDR) and inhibition of homologous recombination (HR) repair (Ali et al. 2018). RYBP, through its Npl4 zinc finger (NZF) domain is found to bind K63-diubiquitin chains, which often are seen around DNA double strand breaks (DSBs). RYBP is removed quickly from surrounding chromatin upon DSB recognition through its own K48 ubiquitination by RNF8, an E3 ubiquitin ligase assisted by the segregase activity of p97. The removal of RYBP from chromatin allows for the recruitment of repair complexes to the damaged DNA sites; however, this removal is not dependent on ncPRC1. This is exemplified by the finding that RYBP overexpression inhibited BRCA1 complex formation and recruitment to DSBs through competitive binding with the DSB site, ultimately leading to decreased HR repair (Ali et al. 2018). RYBP overexpression also inhibited HR through inhibiting ataxia telangiectasia mutated (ATM) kinase activity and recruitment to damaged DNA, important for early DDR (Maybee et al. 2022). Because HR repair is the most accurate double strand break DNA repair mechanism and DSBs are easily recognizable, RYBP poses a potential relevance in cancer or cancer therapeutics, as decreased HR repair would, ostensibly, sensitize cells to DNA damage-based chemotherapies and promote cell death. These combined results

indicate that ncPRC1, through its inclusion of RYBP, is highly significant for epigenetic regulation and subsequent chromatin compaction and initiates gene repression and regulation in the nucleus.

Cancer-Related Phenotypic Effects of RYBP

Through its roles in transcriptional regulation and PRC1-independent functions, RYBP exerts a variety of effects on different cell phenotypes that are relevant to cancer, including cell proliferation, apoptosis, motility, and invasion. RYBP has been elucidated as a tumor suppressor in certain cancers while playing an oncogenic role in others, demonstrating that its regulation is highly important and cell type-specific in a way that deserves extensive investigation. A full understanding could elicit therapeutic tactics involving RYBP as a novel drug target or as a prognostic marker. RYBP is typically down-regulated in tumor cells, but specific cancers like Hodgkin's lymphoma and T-cell lymphoma increase RYBP expression (Sanches-Beato et al. 2004; Sasaki et al. 2011), indicating there are contexts in which RYBP behaves as an oncogene. Furthermore, the specific effects that RYBP expression has within varying cancers (proliferation, invasion, migration, and apoptosis) is highly context dependent. This demonstrates cell type-specific functions of RYBP and highlights the need for individualized assessments of each type of cancer for context-dependent effects of RYBP dysregulation.

Proliferation

Proliferation is a highly important and regulated mechanism in normal cells, and its deregulation is a major hallmark by which tumors become populated. Zhao et al. (2019) speculated that e26 transformation specific-1 (ETS1)-mediated inhibition of cellular proliferation in HeLa cervical cancer cells was achieved through its binding and regulation of RYBP. ETS1 binding to the *RYBP* promoter stimulates its transcription and subsequent translation, and *RYBP* contains multiple binding sites for ETS1 within its promoter region.

The multiple binding sites provide an opportunity for RYBP expression to be fine-tuned by regulatory cues, such as modulation in ETS1 expression. As ETS1 is a transcription factor associated with suppressing tumor cell proliferation, this effect was achieved, at least in part, through RYBP promoter binding and regulation, possibly aided by p21 (Zhao et al. 2019). Moreover, cervical cancer is often seen to have low levels of RYBP due to frequent deletions on chromosome band 3p, where RYBP is encoded. This leads to worse survival rates and chemoradioresistance (Lando et al. 2013). Similarly, in prostate cancer, 3p deletions, and thus decreased RYBP levels, are common. These deletions were correlated with a higher tumor stage (Krohn et al. 2013). Induced expression of RYBP in prostate cancer inhibited tumor cell proliferation and growth, highlighting the tumor suppressive effects of RYBP in prostate cancer (Krohn et al. 2013).

RYBP expression is downregulated in esophageal squamous cell carcinoma (ESCC), and rescuing RYBP's expression was seen to inhibit ESCC proliferation by inhibiting DNA replication (Ke et al. 2020). RYBP most importantly decreases the level of CDC6 and CDC45, along with MCM3 and MCM5. CDC6 and CDC45 are involved in DNA replication initiation in the G1-S phase transition (Ke et al. 2020) demonstrating that the tumor suppressive effects of RYBP occur through a multitude of molecular mechanisms.

The epidermal growth factor receptor (EGFR) protein and its associated signaling pathways are known to be involved in cellular mechanisms such as proliferation, differentiation, and epithelial-mesenchymal transition (EMT). In lung cancer, Dinglin et al. (2017) found that RYBP overexpression led to decreased cell proliferation, migration, and invasion, most likely through suppressing EGFR-associated pathways. MicroRNAs (miRNAs) are a class of small noncoding RNAs (around 20 nucleotides) that affect gene expression typically by binding the untranslated regions (UTRs) of their target mRNAs (O'Brien et al. 2018). They have also recently been reported to be involved in tumor cell regulation and function. MiR-769-5p and miR-125b-5p in gastric carcinoma were

upregulated and shown to target and inhibit RYBP, and their expression was found to be associated with increased cell proliferation and worse prognosis (Luan et al. 2020, Jin et al. 2021).

Apoptosis

Apoptosis, a form of controlled cell death, is a crucial cellular mechanism important for development, aging, and proper immune response (Kerr et al. 1972). Apoptosis typically involves activating the caspase cascade, breaking down DNA and proteins within the cell, condensing the nucleus and cytoplasm into fragments, and phagosome/lysosomal uptake and degradation (Kerr et al. 1972). Apoptosis may be achieved by either the intrinsic or extrinsic pathways. The intrinsic, or mitochondrial, pathway is utilized upon recognition of DNA damage or depletion of necessary cellular survival factors within a cell. The tumor suppressor p53 is activated, leading to transcription of mitochondrial pro-apoptotic Bax and BH3-only family proteins and suppression of anti-apoptotic Bcl2, causing a release of cytochrome c from the mitochondrial intermembrane space into the cytosol. Cytochrome c binds with pro-caspase-9 to form an apoptosome, leading to caspase-9 activation and subsequent activation of effector caspases, like caspase-3 (Al-Aamri et al. 2021). Meanwhile, the extrinsic pathway, or death receptor pathway, leads to cell death due to extracellular conditions. Death receptors from the tumor necrosis factor receptor (TNFR) superfamily bind extracellular molecules, forming the death-inducing signaling complex (DISC) and activating initiator caspase-8 or -10, which in turn activates caspase-3 or mitochondrial outer membrane permeabilization (MOMP) (Al-Aamri et al. 2021). Activated caspase-3 subsequently induces apoptosis through promoting nuclear fragmentation, membrane blebbing, and through activating DNA damage by inhibiting poly(ADP-ribose) polymerase (PARP) (Porter and Jänicke 1999) (Figure 2). PARP is involved in DNA repair and its inhibition and subsequent accumulation of DNA damage promotes apoptosis (Skidmore

et al. 1979). Apoptosis is often dysregulated or turned off in cancerous cells, allowing for the tolerance of stressors that accompany uncontrollable division. This ensures that cancer cells do not die before they populate the tumor (Wong 2011). RYBP has been found to interact with and regulate various components of the apoptotic machinery.

In intrinsic apoptosis, one important interaction of RYBP is with the Bcl6 corepressor (Bcor) complex, which targets genes such as *TP53* and *Cyclin D2* in lymphoma cells (Gearhart et al. 2006). RYBP also inhibits the mouse double minute 2 (MDM2) oncoprotein from ubiquitinating and degrading p53, thereby liberating p53 to activate the intrinsic apoptotic pathway (Chen et al. 2009). RYBP also functions within the extrinsic pathway of apoptosis. In yeast, RYBP interacts with FADD, caspase-8, and caspase-10 while also enhancing the formation of DISC in the cytoplasm. This same relationship has been observed for homologous mammalian proteins and shows RYBP's participation in encouraging CD95-mediated apoptosis (Zheng et al. 2001). Tan et al. (2017), in osteosarcoma and colorectal carcinoma cells, found that RYBP has a nuclear localization signal (NLS) responsible for its transport into the nucleus. When a mutant RYBP missing its nuclear localization signal was introduced into a cell, RYBP was, predictably, restricted to the cytoplasm. This cytoplasmic mutant RYBP interacted with p53, caspase-8, and Hip1 protein interactor (HIPPI) in the cytoplasm and induced tumor apoptosis even more effectively than its nuclear counterpart (Tan et al. 2017). Nuclear RYBP also interacted with a DED-containing DNA-binding protein (DEDD) and facilitated DEDD-induced apoptosis (Zheng et al. 2001) (Figure 2).

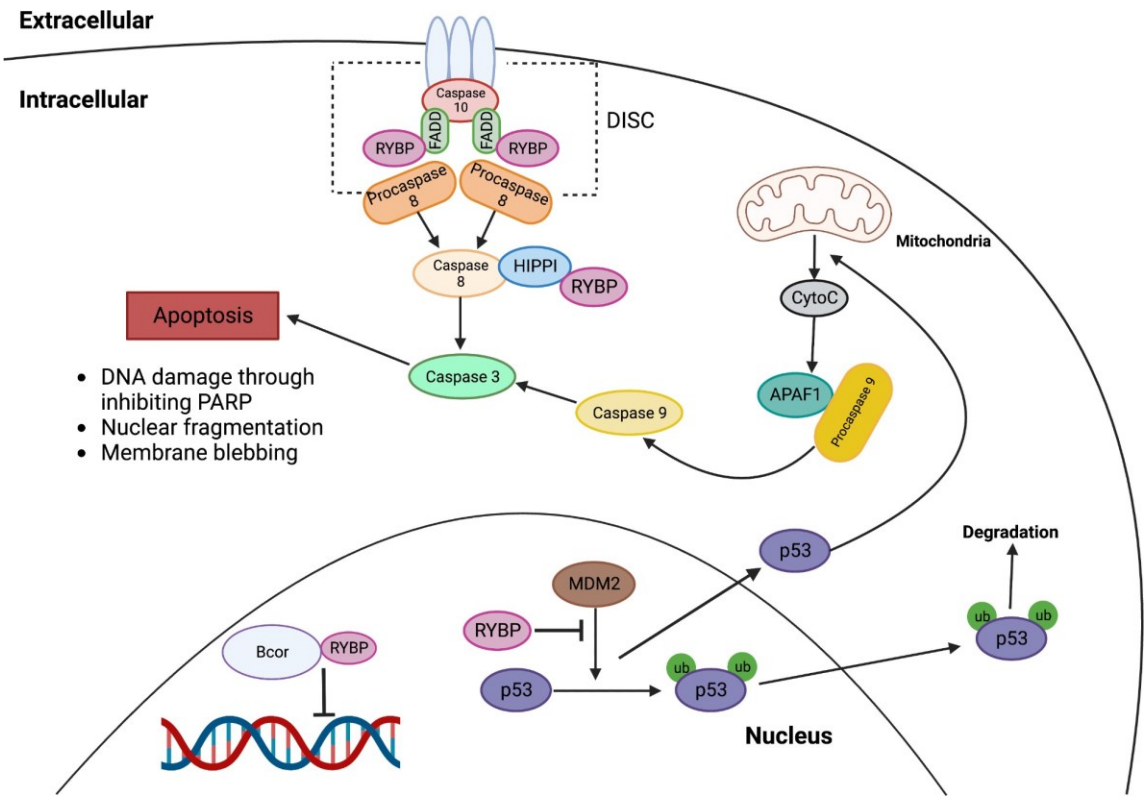

Figure 2. RYBP involvement in apoptotic pathways. In the extrinsic pathway, RYBP can interact with FADD, caspase-8, and caspase-10, enhancing the formation of DISC and promoting apoptosis. Also in the cytoplasm, RYBP can interact with HIPPI to promote apoptosis through caspase-8. In the intrinsic apoptotic pathway, RYBP can interact with the Bcl6 corepressor (Bcor) complex and inhibits MDM2 ubiquitination and degradation of p53, thereby allowing p53 to stimulate apoptosis (Created with BioRender.com, adapted from Wang et al. 2015).

Motility and Invasion

Motility and invasion mediate the most lethal hallmark of cancers: local and regional dissemination and distant metastasis. Although distant metastasis is uncommon in GBM patients due to their short survival, the molecular mechanisms involved are still highly relevant as they are commonly adopted in GBM to support local spreading and

invasion into surrounding healthy neural tissue. In order to begin this process, cancer cells must undergo cytoskeletal rearrangements and lose cell-cell adhesions that otherwise keep the cells immobile (Novikov et al. 2021). This is marked by the epithelial-to-mesenchymal transition (EMT), whereby cells undergo changes in shape and lose their polarity and symmetry and convert to a more mesenchymal-like state, becoming mobile (Friedl and Alexander 2011; Zhou et al. 2016). One major indicator of this transition is a cell's reduction of E-cadherin, which is used to enhance cell-cell contact (Novikov et al. 2021). An accompanying increase in Snail or Slug, transcriptional repressors of E-cadherin, has also been reported to support EMT (Zhou et al. 2016). An increase in N-cadherin is typically seen following EMT and associated with increased tumor cell migration and invasion (Cao et al. 2019). N-cadherin promotes the expression of matrix metalloproteinases responsible for degrading surrounding membranes. N-cadherin also forms a complex with β-catenin to make up parts of the actin cytoskeleton. Tumor cells frequently degrade these complexes leaving the beta-catenin free to translocate into the nucleus, resulting in further MMP production and enhanced invasive capabilities (Cao et al. 2019). Vimentin, a structural intermediate filament, is also frequently found to be increased in cancer cells, and its expression is attributed to helping cancer cells undergo mechanical stresses involved in moving and invading (Liu et al. 2015). Another mechanism intricately involved in cancer cell migration and invasion is aberrant growth factor signaling, such as with epidermal growth factor receptors (EGFR) (Witsch et al. 2010). This aberrant signaling can also lead to enhanced EMT (Witsch et al. 2010; Tong et al. 2018).

Induced RYBP expression decreased breast cancer cell growth, migration, and invasion (Zhou et al. 2016). The expression of RYBP was also associated with an increase in epithelial E-cadherin and a reduction in Snail, suggesting it exerted its phenotypic effects through suppression of EMT. In lung cancer and anaplastic thyroid cancer (ATC),

RYBP was downregulated (Dinglin et al. 2017; Tong et al. 2018). Meanwhile. RYBP's overexpression caused a decrease in EGFR and ERK1/2 phosphorylation and activation, ultimately inhibiting lung cancer and ATC cell proliferation and invasion (Dinglin et al. 2017; Tong et al. 2018). As mentioned above, miR-125b-5p negatively regulated RYBP in gastric cancer, and this reduction in RYBP may have mediated the increased gastric cancer cell invasiveness associated with miR-125b-5p (Jin et al. 2021). In hepatocellular carcinoma (HCC), RYBP overexpression led to inhibition of migration and invasion of HCC cells, possibly by up-regulating expression of an anti-invasive microRNA, miR-769-5p (Xian et al. 2019).

Chapter Two

Materials and Methods

Cell Lines and Maintenance

Two different human cell lines, U-118 and T98G, were obtained from ATCC. These have both been commonly used for in vitro cell culture experiments in GBM research. The T98G cell line is derived from a malignant brain tumor that is thought to be GBM in origin. U-118 is a widely used and accepted cell culture model for GBM studies and is derived from a known human GBM tumor. By using both T98G and U-118 cells, we ensured our results were not an artifact of only one cell line.

To grow and prepare the individual cell lines, we thawed cryopreserved cells and cultured them to 80-90% confluence. These populations were maintained in a 37 ^{o}C incubator with 5% CO_2 and 95% humidity. Subculturing was done according to the specific cell line's protocol in 1:3 to 1:5 ratios for U-118 and T98G cells, respectively. O.25% Trypsin-EDTA solution from ATCC® was used to dissociate cells. A complete growth medium of EMEM, supplemented with 10% fetal bovine serum (FBS) was used for T98G cells, and complete DMEM supplemented with 10% FBS was used for U-118 cells. All media was supplemented with 1% penicillin/streptomycin solution to reduce the likelihood of bacterial contamination and 1% L-glutamine to aid in cell growth. Cells were grown on standard tissue culture plastic.

Viral Transduction

We generated cell lines with stably manipulated RYPB expression by transducing cells using lentivirus (OriGene) that encoded puromycin resistance and a green fluorescent protein (GFP) marker in either an empty control vector or an RYBP-expressing vector, in which RYPB is conjugated to GFP and its expression is driven by the cytomegalovirus (CMV) promoter (Figure 3).

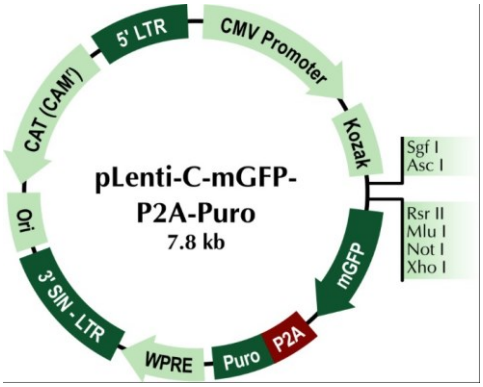

Figure 3. Lentiviral vector schematic of the control lentivirus. The RYBP coding sequence was inserted into the multiple cloning site downstream of the CMV promoter and the Kozak sequence by the manufacturer. The RYBP coding sequence is fused to the GFP coding sequence.

We first optimized the multiplicity of infection (MOI) to find the most effective, minimal amount of lentiviral particles needed to effectively transduce 100% of treated cells. MOI was optimized for each cell line with the control virus by testing MOIs of 5, 10, and 20 transducing units per cell and observing GFP expression after 48-72 hours. MOI was determined for both U-118 and T98G cell lines.

$$\text{Desired MOI} = \frac{\text{Total transducing units needed}}{\text{Total number of cells per well}}$$

$$\text{Total mL of lentiviral particles to add to each well} = \frac{\text{Total transducing units needed}}{\text{Transducing units/mL}}$$

$$\text{Therefore: mL of lentiviral particles to add to each well} = \frac{\text{Number of cells per well x MOI}}{\text{Transducing units/mL}}$$

Once the lentiviral transduction protocol was optimized, lentiviral particles were thawed on ice and added at the determined optimal MOI (MOI of 5 for U-118s and MOI of 10 for T98Gs) to 500 µL culture medium in a 6-well plate for each cell line along with polybrene at 8 µg/mL. Polybrene was added to enhance the success rate of lentiviral transductions through neutralizing the cell surface and increasing the binding ability of the viral capsid protein to the cell. Cells were incubated with virus for 24 hours, and then the

media was changed the next day and replaced with 2 mL normal complete medium and left overnight. The cells were then subjected to puromycin selection.

Prior to selection, kill curve experiments were performed to determine the correct amount of puromycin to add for each cell line. To do this, we plated $5x10^4$ cells per well in a 24-well plate with 500 µL complete media. Puromycin was added to different wells at various concentrations (0.5 to 10 µg/mL) and the cell viability was observed each day for 5 days, changing the media every three days. The lowest concentration of puromycin needed to cause total cell death after five days was then used to select virally transduced cells.

Following lentiviral transduction and puromycin selection, cells were observed under fluorescent light using a confocal microscope to confirm GFP expression. GFP expression was also confirmed every time frozen stocks of stable cells were thawed and again at the end of every experiment.

Protein Isolation and Quantitation

Following puromycin selection, transduced cells were assayed to confirm ectopic RYBP expression. Cells were washed three times with cold 1X PBS on ice and scraped utilizing a sterile cell scraper. Cells were resuspended in 500 µL cold 1X PBS. The cells were pelleted by centrifuging at 8000 x g at 4 °C for one minute before removing the supernatant and adding 100 µL of RIPA buffer containing a 1:10 dilution of protease inhibitors. The RIPA buffer lyses cells and the protease inhibitor mixture prevents protein sample degradation. Following a 30 min incubation on ice, samples were centrifuged at 14,000 RPM at 4 °C and the supernatant was quantified.

We used the Modified Lowry Protein Assay to quantify the amount of protein present in our samples. Ten dilutions, including a blank, were prepared from BSA standards of known concentration, ranging from 1 to 1500 µg/mL. For both standards and

unknown samples, 20 µL was added to individual test tubes and incubated for 10 min with 1 mL Modified Lowry Reagent. We then added 100 µL 1X Folin-Ciocalteu Regent to each reaction, incubated 30 min in the dark, and measured absorbance at 750 nm. A standard curve was determined by plotting the absorbance values of the diluted standards against their known concentrations in µg/mL generating a line of regression. The concentration of each isolated unknown protein sample was then calculated using the standard curve.

SDS-PAGE and Western Blot

We loaded 15 µg of quantified protein samples on a 10% polyacrylamide gel and electrophoresed at 150 V for 1-1.5 h. Proteins were transferred to a nitrocellulose membrane at 100 V for 1 h on ice. Membranes were blocked for 1 hour at room temperature using 5% non-fat milk. Membranes were then cut to allow for probing of multiple proteins at once. After blocking and cutting, we probed the membranes with a primary antibody against proteins of interest, washed the membranes in TBST, and then probed with an HRP-conjugated secondary antibody. After additional TBST washes, we visualized and imaged bands using enhanced chemiluminescence (ECL) reagents. Western blotting was used to (1) confirm ectopic RYBP expression in virally transduced cells using a primary antibody against RYBP (Cell Signaling Technology Cat# 41787) and (2) measure differences in levels of cleaved caspases and cleaved PARP, markers of apoptosis, as well as markers of epithelial-to-mesenchymal transition (EMT) between RYBP-expressing and control cells (n=1). RYBP was detected using an anti-RYBP primary antibody. The apoptosis antibody kit obtained from Cell Signaling Technology (Cat# 9915) was used, as it includes primary antibodies against cleaved and non-cleaved Caspases-3 and -7 (markers of middle stage apoptosis), caspase-9 (a marker of early apoptosis), and PARP (indicative of late apoptotic cells). The EMT markers included in the

Cell Signaling Technology Epithelial-Mesenchymal Transition Antibody Sampler Kit (Cat# 9782) were used to detect vimentin, N-Cadherin, E-Cadherin, Slug, Snail, and β-Catenin.

WST-1 Proliferation Assays

We performed WST-1 proliferation assays with all infected GBM cell lines (U-118 and T98G Control and RYBP populations) to elucidate any differences in cell growth occurring as a result of ectopic RYBP expression according to the Millipore Sigma WST-1 Assay Kit protocol. The WST-1 reagent is digested by mitochondria, producing a colorimetric reaction. This change indicates the number of cells present and is based on the assumption that higher cell numbers will have more mitochondria, thereby producing more robust colorimetric reactions. However, the WST-1 reaction kills cells, so new populations, all established on day 0, were utilized for each subsequent day. Initially, we seeded $2.5x10^3$ or $5x10^3$ cells per well in a 96-well plate (Figure 4). Each cell line was plated in triplicate six times (to be measured on days 0-5) as depicted in Figure 4 in a single row of wells. Complete media without cells was added to six wells in another row for standardization. Every day at 24 h intervals, 10 µL of WST-1 reagent was added to three wells of each cell line condition and one media well and allowed to incubate at 37 °C. After 4 h, absorbance at 450 nm was recorded using a microplate reader. We also measured absorbance at 750 nm as a reference wavelength to account for background signals and subtracted this reference value from the absorbance reading at 450 nm. Overall, cells were measured over five days and the average adjusted A_{450} value for each group compared at every time point.

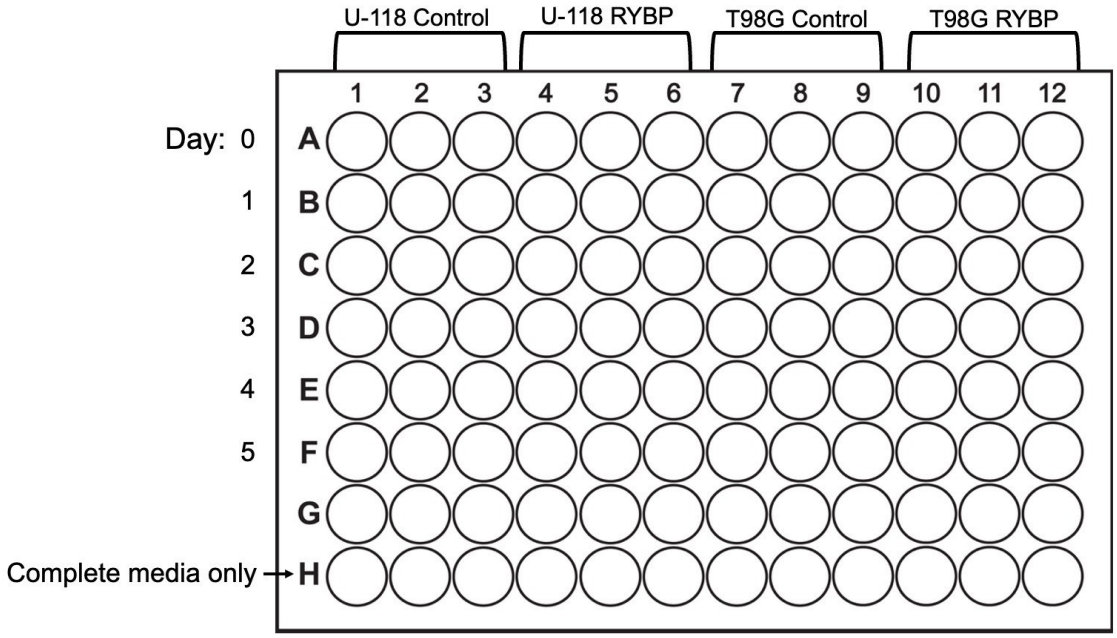

Figure 4. WST-1 Proliferation Assay. Example set-up of WST-1 Assay 96-well plate for both control and RYBP expressing T98G and U-118 cells.

Wound-Healing Assays and Matrigel Invasion Assays

Wound healing assays were performed to observe differences in the migration of RYBP-expressing vs control cells of each virally transduced parental cell line (U-118 and T98G). A confluent flask of cells was scratched across the monolayer. These flasks were then observed under a microscope at 100X magnification and imaged every 12 to 24 h for the T98Gs and every 24 to 48 h for the U-118s to visualize the area of the wound that was closed in multiple fields of view along the scratch. Areas were quantified using Image J software and differences in wound area were averaged and compared between groups. After each scratch image was opened in ImageJ, they were turned into 8-bit images and the image threshold was reset. Under Process-FFT, we used the Bandpass filter and accepted automated formatting. We then adjusted the image threshold top bar (base value) to 60 with the bottom bar (top value) based on the images and it was applied. A

Minimum Filter was used, and the radius was set to 7.0 pixels. The wand tool was then used to click inside and insert lines along the edges of the scratch. After setting the scale in ImageJ to convert from pixels to μm, we then measured the area of the wounds.

To measure differences in the invasiveness of RYBP-expressing and control cell populations, a Matrigel-coated Invasion Chamber from Corning was utilized according to the manufacturer protocol. Briefly, $2.5x10^4$ cells were plated into an upper chamber in 500 μL serum-free media. The chamber was then placed into 750 μL serum-rich media in the well of a 24-well plate, creating a chemoattractant gradient that stimulated cell motility (Figure 5). A Matrigel coating separated cells from the serum-rich media in the lower chamber. The Matrigel coating provided a matrix that cells must degrade to invade in an attempt to reach the serum-rich media. This models cancerous cells' ability to invade through extracellular matrices to nearby tissues, a major concern for aggressive tumor types like GBM. Prior to plating cells, Matrigel inserts were rehydrated and the chemoattractant was added to the wells in which the chambers are placed. Once plated, cells were incubated overnight at 37 °C and 5% CO_2 for 24 to 48 h. Then, cells that were unable to invade were scrubbed from the upper chamber using a cotton swab. Meanwhile, cells that invaded through the Matrigel were fixed on the membrane in 10% formalin for 3 min, washed with 1X PBS, and stained with 0.1% crystal violet for 10 min. Chambers were washed in distilled water and dried overnight at room temperature. The number of invading cells was counted with a microscope at 100X magnification in 5 fields of view for each chamber. In each experiment, we counted invasive cells in three chambers for each cell population and performed the experiments a total of three times with both U-118 and T98G cells. The average number of invading cells per chamber was determined for each cell line and compared across populations.

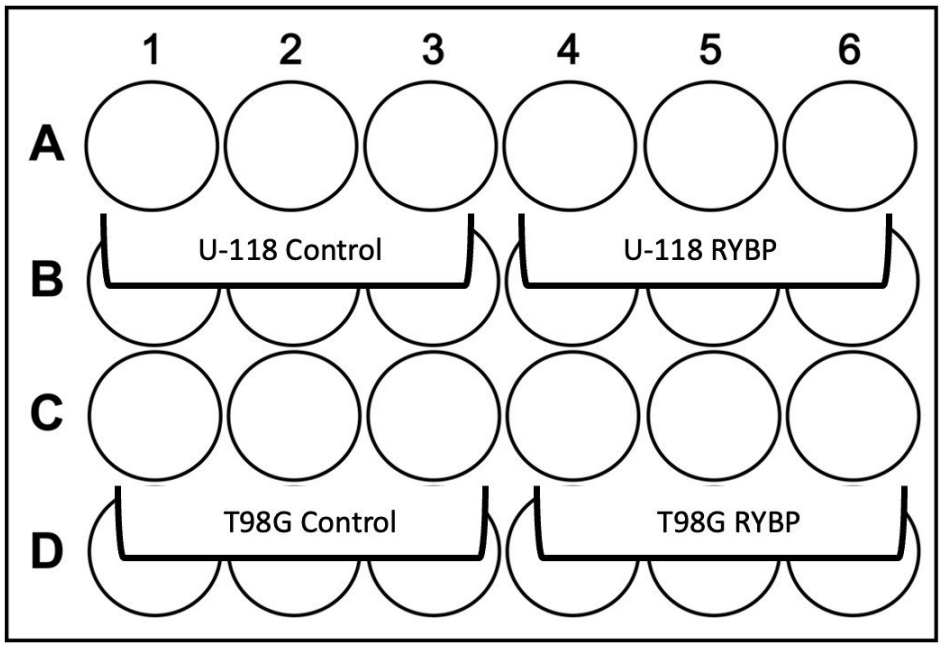

Figure 5. Matrigel Invasion Chamber. Example Matrigel Invasion Chamber 24-well plate. A total of $2.5x10^4$ cells were loaded per chamber for the two populations (control and RYBP) of a single cell line (U-118 and T98G).

Statistical Analysis

Means were averaged from experiments performed in triplicate and repeated three times to ensure accuracy and reliability; n=3 for wound healing and invasion assays. To determine if there was a significant difference in means of data collected from invasion (Boyden chamber) assays, we used a two-tailed, unpaired T test. Differences were considered statistically significant if $P \leq 0.05$. For wound healing assays, we used a one-way ANOVA test, because the average wound area for each group of cells was measured at multiple time points, and thus the means of more than two groups were being compared.

Prior to performing the ANOVA, we performed an F-test to determine if the variance between samples was significantly different. Since there was no significant

difference in the variances, we proceeded with the ANOVA. To perform the ANOVA, we determined a p-value and an F statistic. The F statistic is based on the relationship between the variance within groups and the variance between groups. Differences in means were considered statistically significant if $P \leq 0.05$. A post-hoc test determined which groups are responsible for the statistical differences in means. A Tukey's post-hoc test was used, as we wanted pairwise comparisons between each group.

Chapter 3

Results

Generation of Stable Cell Lines

We hypothesized that RYBP would exert tumor suppressive effects in GBM cells. To begin testing this hypothesis, we used lentivirus to establish stable U-118 and T98G GBM cell lines with induced mGFP or mGFP-RYBP expression. Viral transduction conferred puromycin resistance and puromycin was included in cell culture media to select for colonies that were infected. Therefore, we first performed kill curve experiments to find the appropriate amount of puromycin needed for each cell line (data not shown). The optimal puromycin concentration for selecting U-118 cells was 0.75 µg/mL. In T98G cells, the concentration was 1.0 µg/mL. We also determined the optimal multiplicity of infection (MOI) for each cell line. For U-118 cells, we identified an MOI of 5, and for T98G cells, we identified an MOI of 10 to be optimal (data not shown).

Following lentiviral transduction with the optimal concentration of virus, U-118 and T98G cells were expanded under optimal puromycin selection and imaged for GFP fluorescence (Figure 6A) to confirm successful uptake of the lentiviral vectors. We then used Western blot analysis to ensure ectopic expression of RYBP (32 kDa) and found we had successfully induced stable expression in both U-118 and T98G cells compared to GFP-only controls (Figure 6B). The use of the term stable is supported here by prolonged GFP-RYBP expression, as confirmed by continued GFP expression when observed under fluorescent light and presence of RYBP protein as seen on Western blots over twenty passages post transfection.

RYBP Expression Significantly Inhibited GBM Cell Migration and Invasion

RYBP frequently plays a tumor suppressive role in cancers (Lando et al. 2013; Tong et al. 2018; Ke et al. 2020) and ectopic RYBP expression has been linked to reduced breast cancer and HCC migration (Zhou et al. 2016; Xian et al. 2019). Thus, we hypothesized that induced RYBP expression would lead to reduced migration in U-118

and T98G GBM cells. To assess RYBP's effect on GBM migration, we performed wound-healing assays where perpendicular scratches were introduced across confluent cells in a 6-well plate and allowed to close. The wounds were imaged at 0-, 24-, and 48-hours for U-118 cells and at 0-, 12-, and 24-hour time points for the T98G cells (Figure 7A and C, respectively). Wound area (μm^2) was then quantified using ImageJ. Upon comparisons, RYBP expression significantly inhibited the ability of both U-118 (Figure 7B, $P = 1.947 \times 10^{-89}$) and T98G cells (Figure 7D, $P = 2.338 \times 10^{-68}$) to close the wound at all time points, as determined by one-way ANOVA and Tuckey's post-hoc test. Importantly, there was no difference in starting wound area between RYBP-expressing and control cells ("time 0").

Mechanisms mediating migration are closely associated with those of invasion in cancer cells. While migration demonstrates the cell's loss of attachments and ability to move, invasion is an active process that requires cells to degrade the extracellular matrix, thus allowing increased migration into surrounding healthy tissue or metastasis. To test the hypothesis that RYBP also plays a tumor suppressive role in GBM through restricting invasion, Boyden chamber invasion assays were used where the number of cells invaded through the Matrigel insert were counted and compared between control and RYBP-expressing cells (Figure 8A). Ectopic RYBP expression led to significant reductions in the number of invaded cells per chamber relative to controls in U-118 ($P = 0.007658$) and T98G cells ($P = 8.229 \times 10^{-5}$) (Figure 8B).

RYBP Expression Altered EMT and Apoptosis Marker Levels

The mechanism behind cancer cells' acquisition of enhanced migratory and invasive capabilities has often been attributed to cells undergoing EMT (Cao et al. 2019). We hypothesized that induced RYBP expression would inhibit EMT in GBM by increasing epithelial E-cadherin expression and decreasing levels of mesenchymal markers, such as Snail, Slug, β-catenin, vimentin, and N-cadherin. Utilizing Western blots, we observed

what appeared to be a decrease in vimentin upon RYBP expression in both U-118 and T98G cells as expected (Figure 9). Surprisingly, however, N-cadherin levels appeared to have increased upon ectopic RYBP expression across U-118 and T98G cells. No expression was detected for E-cadherin, Slug, Snail, or β-catenin in either control or RYBP infected U-118 or T98G cells (data not shown).

Many tumor suppressor proteins activate apoptosis. Therefore, we hypothesized that induced RYBP expression in U-118 and T98G GBM cells would lead to increased levels of pro-apoptotic proteins such as activated caspases (-3, -9, and -7) as well as PARP. Preliminary results measuring the levels of apoptotic markers in T98G GBM cells seemingly show increased executioner caspase-3 activation (seen by an apparent increase in cleaved caspase-3 in RYBP-expressing cells compared to control), indicating increased levels of apoptosis upon ectopic RYBP expression (Figure 10).

Assessment of GBM Proliferative Potential upon RYBP Expression

Another dysregulated mechanism in cancer is increased cellular proliferation, leading to increases in tumor population. We hypothesized that ectopic expression of RYBP in GBM cells would reduce proliferation. To test this, WST-1 assays were employed. During the first replicate it was found that the plate reader reached its max absorbance values when measuring after day two. To account for this, we reduced the number of plated cells to $2.5x10^3$, but still faced the same issue. Due to the inability of the plate reader to obtain readings, results for these assays were inconclusive (data not shown).

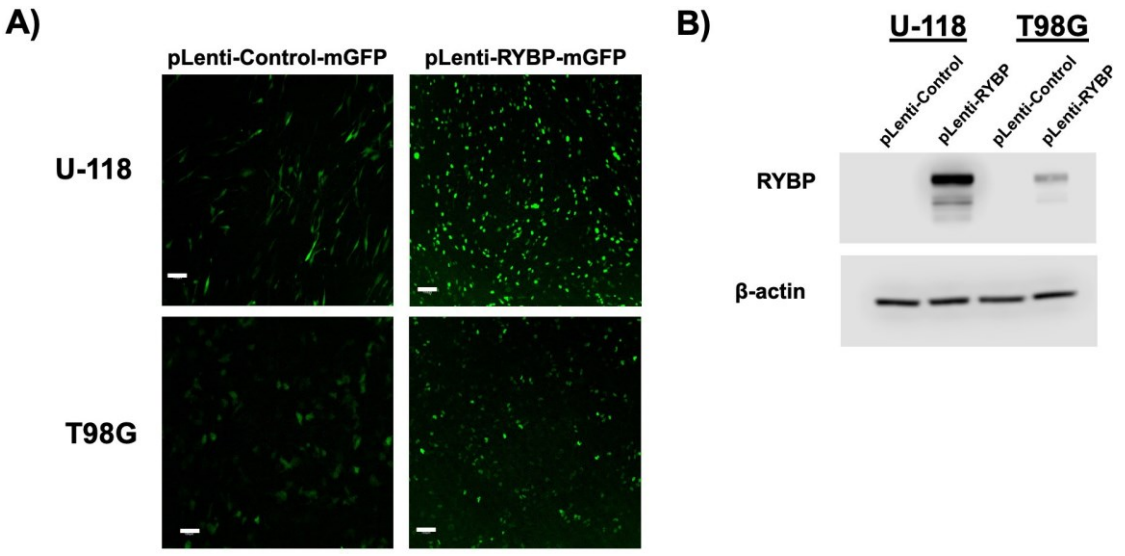

Figure 6. Generation of Lentivirally-Transduced U-118 and T98G Cells. (A) T98G (upper panels) and U-118 cells (lower panels) were transduced with a GFP-expressing control lentivirus (pLenti-Control-mGFP) or a lentivirus expressing RYBP conjugated to GFP (pLenti-RYBP-mGFP vector). Following lentiviral transduction, GFP expression was detected using a confocal fluorescent microscope. Scale bar = 100 μm. **(B)** Western blot results confirming RYBP-GFP expression upon lentiviral transduction in U-118 and T98G cells. β-actin was used as a loading control.

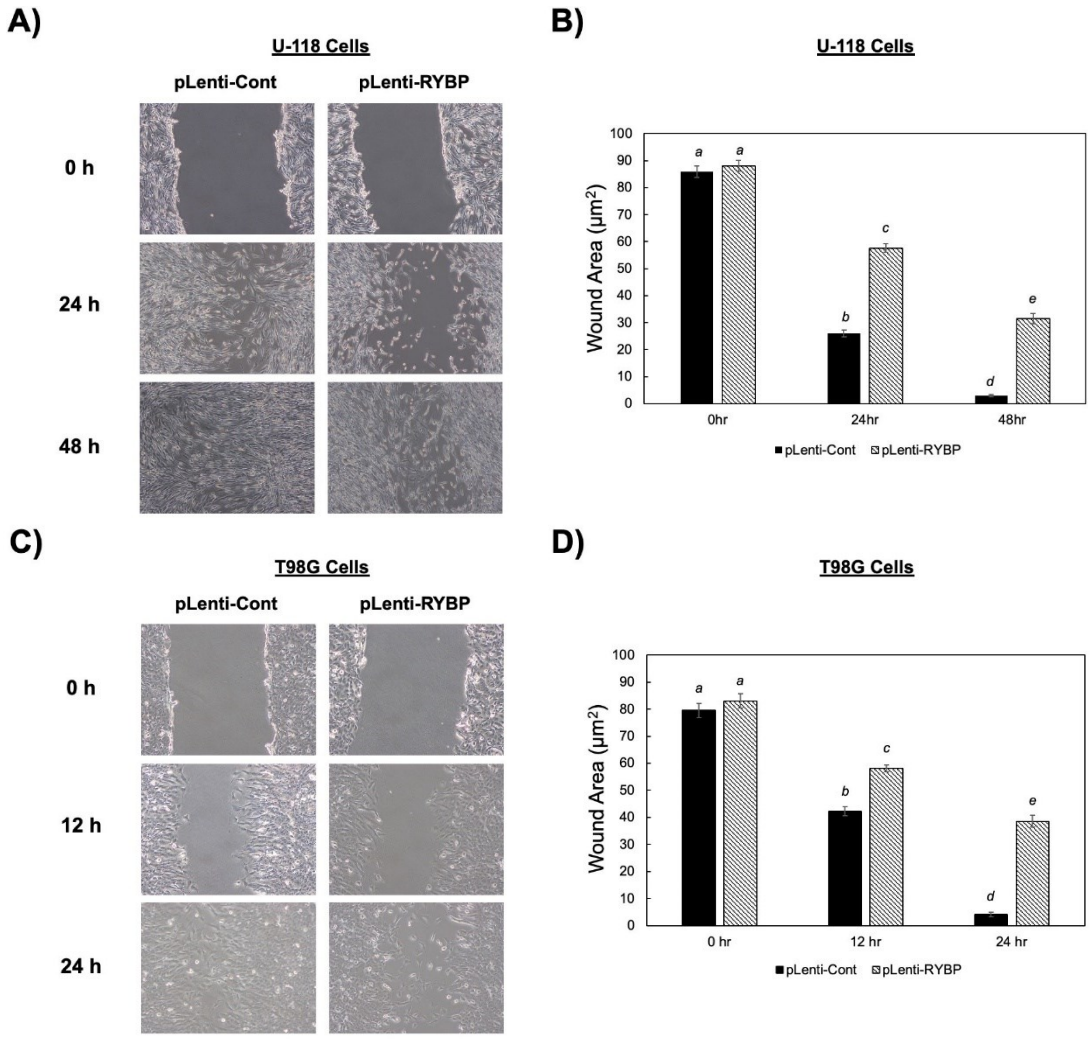

Figure 7. Ectopic RYBP Expression Significantly Decreases GBM Cell Migration. Representative images from wound-healing assays show the wound area (μm^2) and closure in U-118 **(A)** and T98G **(C)** cells infected with either control or RYBP-expressing virus. T98G scratches were imaged at the 0-, 12-, and 24-hour time points, and U-118 scratches were imaged at the 0-, 24-, and 48-hour time points at 100X magnification. Images were quantified using ImageJ. Graphs represent the mean wound area ±SEM from three experiments with each condition in triplicate for U-118 **(B)** and T98G **(D)** cells. Letters indicate statistical differences between groups as determined by a one-way ANOVA and Tukey post-hoc test. For U-118 cells, $P = 1.947 \times 10^{-89}$ **(B)**, for T98G cells $P = 2.338 \times 10^{-68}$ **(D)**.

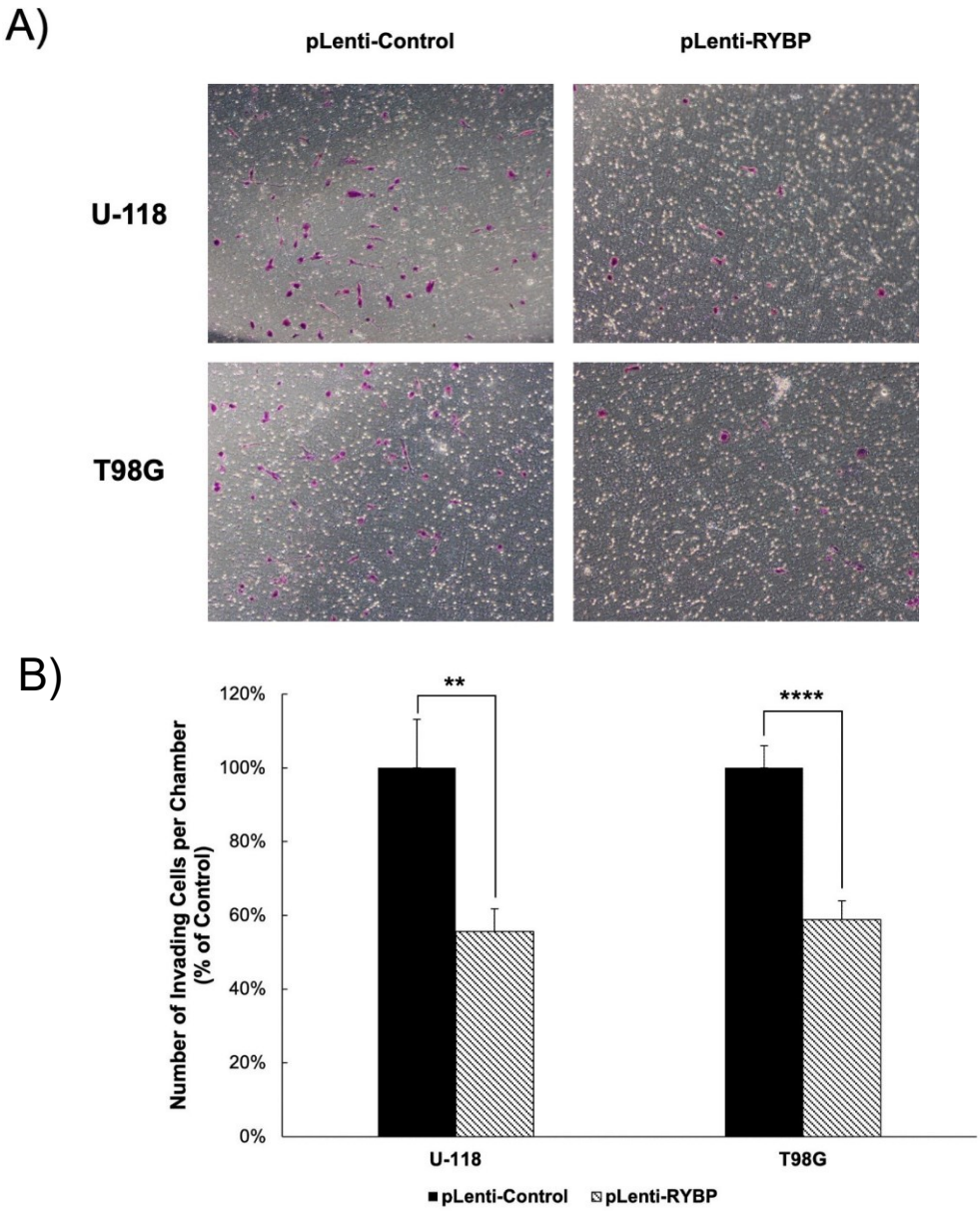

Figure 8. Ectopic RYBP Expression Significantly Decreases GBM Cell Invasion. In both U-118 and T98G control and RYBP infected cells, invading cells were counted in Matrigel-coated Boyden chamber assays. **(A)** Representative images of control and RYBP expressing U-118 and T98G cells show the invading cells (purple) at 100X magnification. **(B)** Graphs represent the mean ±SEM from three experiments with each condition in triplicate. **, p ≤0.01; ****p ≤0.0001 as determined by an unpaired, two-tailed t-test.

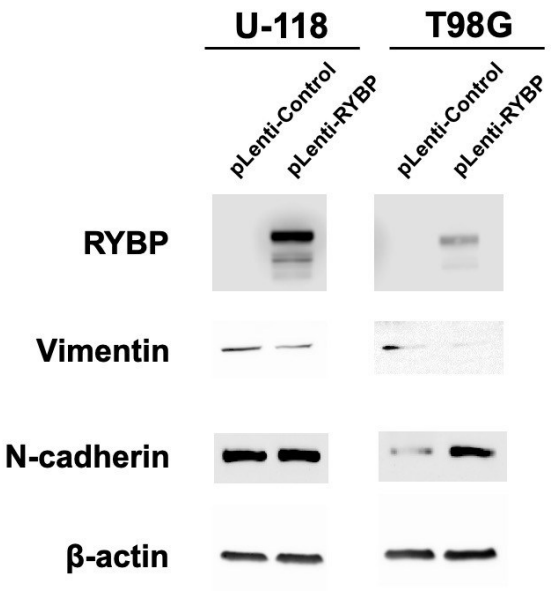

Figure 9. RYBP Alters EMT Marker Levels. In U-118 and T98G control and RYBP infected cells, Western blot analysis confirmed RYBP expression and showed an apparent decrease in vimentin and increase in N-cadherin upon ectopic RYBP expression. n=1. β-actin was used as a loading control.

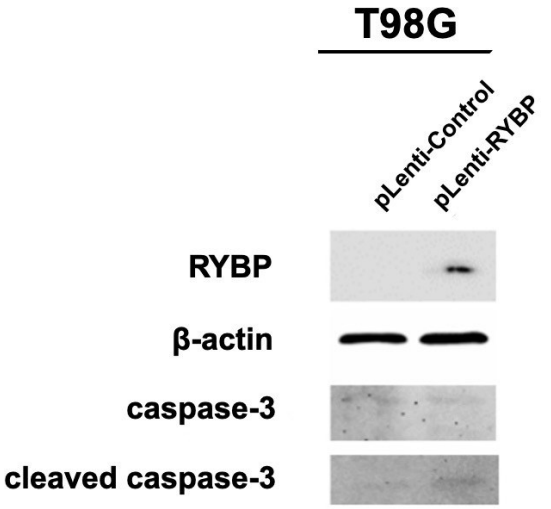

Figure 10. RYBP Alters Apoptotic Marker Levels. T98G control and RYBP cells were analyzed for apoptotic markers including caspase-3 and cleaved caspase-3. n=1. β-actin was used as a loading control.

Chapter Four

Discussion

RYBP is important in many cellular mechanisms and displays aberrant expression profiles in various cancers. Often, RYBP is decreased in cancers and associated with worse prognosis. The experimental induction of RYBP expression in many cancer cells has elucidated a tumor suppressive role of RYBP through the antagonism of multiple cancerous phenotypes, but this can be context specific (Sanches-Beato et al. 2004; Sasaki et al. 2011). Reduced RYBP expression seen in a large portion of GBM patients was associated with worse prognosis, which led us to hypothesize that RYBP may play a tumor suppressive role in GBM (Li et al. 2013). We predicted that forcing ectopic RYBP expression in GBM cells would lead to an increase in apoptosis and a decrease in GBM cell proliferation, migration, and invasion.

We first established cell lines that stably expressed mGFP-Control or mGFP-RYBP constructs and confirmed RYBP expression in U-118 and T98G cells (Figure 6). As seen in the confocal fluorescent images, GFP expression of the U-118 and T98G cells transduced with GFP-only control virus appears all throughout the cell body, indicating ubiquitous cytoplasmic expression (Figure 6A). However, in cells expressing the GFP-RYBP fusion protein, the area of GFP fluorescence is much more limited, possibly supporting previous research that RYBP is typically localized to the nucleus and acts as an important nuclear regulator (Neira et al. 2021). Western blot analysis confirmed ectopic RYBP-GFP expression when probing against RYBP in the lentivirally transduced U-118 and T98G cells. Lack of a band in the control expressing U-118 and T98G cells indicated no endogenous expression of RYBP in these GBM cells. The multiple bands seen with RYBP in Western blot analysis most likely represent the three other RYBP splice variants (Figures 3B and 9). The top band represents the band of interest and is the known full-length active form of RYBP (32 kDa).

RYBP's decreased expression has been implicated in reductions of breast cancer and HCC cell migration (Zhou et al. 2016, Xian et al. 2019). Consistently, through wound

healing assays, we found significant reductions in U-118 and T98G cell migration (Figure 7). RYBP expression has also been significantly associated with reduced invasion of cancer cells from the breast, lung, thyroid, and liver (Zhou et al. 2016; Dinglin et al. 2017; Tong et al. 2018; Xian et al. 2019). Likewise, we observed a significant reduction in the number of invading cells upon ectopic RYBP expression in U-118 and T98G cells (Figure 8), supporting that RYBP has a tumor suppressive role in GBM.

When measuring levels of markers associated with EMT, a process intricately linked to cell migration and invasion, we found a decrease in the mesenchymal marker vimentin (Figure 9). Vimentin is a structural protein that allows cancer cells to tolerate increased amounts of mechanical stress experienced during cell migration and invasion (Liu et al. 2015). A reduction in vimentin upon ectopic RYBP expression supports the idea that RYBP reduces cell migration and invasion through a reduction in EMT. However, the increase in N-cadherin levels upon RYBP expression (Figure 9) was unexpected, as N-cadherin is typically seen as a pro-EMT marker. This could indicate that the molecular mechanisms behind which RYBP operates could be much more complex than initially thought. On the other hand, basal N-cadherin expression is unusually high in neuronal cells (Cao et al. 2019). In glioma cells and glial cells, reduced N-cadherin expression caused loss of cell polarity and other cellular defects, where increased N-cadherin was associated with suppressed glioma cell invasion (Asano et al. 2004; Camand et al. 2012). Together, the increase in N-cadherin we saw could actually be indicative of an alternative mechanism of tumor suppression by RYBP that is either independent of EMT or a contextually distinct EMT program in non-epithelial GBM cells.

Evasion of apoptosis by cancer cells is a hallmark that allows propagation and accumulation of mutations amongst cancerous cell populations. RYBP has been known to interact with apoptotic proteins in the cytoplasm and nucleus (Tan et al. 2017; Neira et al. 2021). It has also been shown that RYBP promotes apoptosis in various cancers

(Gearhart et al. 2006; Chen et al. 2009; Tan et al. 2017). Thus, to study if RYBP had any pro-apoptotic effects in GBM, we performed Western blots for apoptotic protein levels. What appeared to be an increase in cleaved caspase-3 upon ectopic RYBP expression in T98G cells was seen (Figure 10). As caspase-3 is an executioner caspase and indicative that apoptosis is actually occurring, a relative increase in expression would suggest a tumor suppressive role of RYBP in GBM through promoting apoptosis. The confirmation of these results in U-118 cells and results for other apoptotic markers were unable to be finalized due to time constraints. Therefore, the effects of RYBP on the activation of additional caspases, such as initiator caspases (e.g., caspase-9) and other executioner caspases (e.g., caspase-7) still need to be measured. The effects of RYBP on apoptotic effectors, like PARP, are also still unclear. Alternatively, to looking at apoptotic marker levels, TUNEL staining could be used to study apoptosis in GBM cells following RYBP expression as it labels nicked DNA, a characteristic of cells in late stage apoptosis. Given a tumor suppressive role of RYBP in GBM, we would expect that forced RYBP expression would lead to an increase in the number of TUNEL-positive cells that would be observed, indicating increased apoptosis. ANEXIN V and PI staining could also be used to detect cells that are in the early stages of apoptosis, the late stages of apoptosis, or that are necrotic. ANEXIN V stains phosphatidylserine residues that are only exposed on the surface of apoptotic cells. PI stains DNA and therefore only enter cells that have membrane damage, indicative of cells that are in late apoptosis or necrotic. Upon forced RYBP expression in GBM cells, we would expect an increase to be seen in early and late apoptotic cells when compared to control cells.

Proliferation is another important hallmark of cancer that is frequently inhibited upon RYBP overexpression (Krohn et al. 2013; Dinglin et al. 2017; Ke et al. 2020). To test if the same is true for GBM, WST-1 assays were performed. Results were inconclusive. We first performed these experiments using $5x10^3$ cells per well in a 96-well plate, but

found that the absorbance measured by the plate reader was too high to be quantified, even after only two days of growth. Therefore, we reduced the cell density to $2.5x10^3$ cells per well, but similar issues were still observed. The WST-1 method was used because it has been shown to work in past research involving cancer cell lines, including GBM, and is a widely accepted method for proliferation quantification based on colorimetric measurements (Sari et al. 2021). However, an alternative colorimetric based approach could be utilized to measure GBM cell proliferation, such as the MTT assay, which assesses cellular metabolic activity. The trypan blue exclusion assay could also be used as an alternative to the WST-1 assay. Trypan blue staining has the advantage of being able to distinguish cell viability and cellular proliferation. This approach may be advantageous as it only requires counting the cells with a hemocytometer.

Our results support our hypothesis that RYBP is a tumor suppressor in GBM because it activates apoptosis and inhibits GBM cell migration and invasion. One potential pitfall of our research was that a mixed population of cells was used, meaning there will be variation in the number of vector insertions occurring across cells as well as variation in where the vector was inserted in the genome. By isolating and generating single-cell clonal populations, any proliferative advantage conferred due to the lentiviral insertion site or number of insertions would be revealed. However, use of a mixed population still helps support our claim that RYBP is exerting tumor suppressive effects. A mixed population could lead to selection for the cancer cells that best survive, presumably those with the fewest RYBP insertions based on our findings of a tumor suppressive role of RYBP. This would indicate that if cells with low RYBP expression outcompeted the others in our populations, this lower RYBP expression still demonstrated potent tumor suppressive abilities when comparing across control and RYBP expressing cells.

In a continuation of our work, known inducers of EMT could be utilized as a positive control. To induce EMT, a cocktail of myeloid-released growth factors could be used

(Ricciardi et al. 2015). In GBM, the tumor microenvironment is typically hypoxic which recruits in myeloid cells that release growth factors TGF-β, EGF, PDGF, and FGF2. These growth factors initiate EMT by altering transcription of factors that are necessary for EMT induction (Iwadate 2016). By combining these four growth factors and exposing GBM cells, we could induce EMT. Inducers of apoptosis could also be used as a positive control. Cancer cells frequently avoid destruction by shutting down intrinsic apoptotic pathways. Therefore, to induce apoptosis in GBM cells to act as a positive control, Apoptosis Activator 2 from Abcam (ab141227) could be used, as it activates intrinsic apoptosis through cytochrome c and caspase activation.

Future work should explore additional phenotypic effects of RYBP in GBM. Altered GBM cellular metabolism should be observed following ectopic RYBP expression as it supports cellular proliferation and relates to EMT. Cancers, including GBM, are known to rely on glycolysis whether due to the Warburg effect or exposure to hypoxic conditions (Warburg 1925; McKelvey et al. 2021). This leads to the generation of lactate which is acidic. A glycolysis assay that observes acidification could be employed to observe any changes in levels of glycolysis following ectopic RYBP expression. If RYBP plays a tumor suppressive role in altering GBM cell metabolism, we would expect to see less acidification due to decreased glycolysis and lactate production. GBM is also known to need a lot of lipids inside the cell to support growth and proliferation, but the accumulation of free fatty acid can also pose as a challenge for GBM cell survival (Kou et al. 2022). To account for this, GBM often stores excess fatty acid in lipid droplets. Therefore, the mechanisms regulating this process appear to be altered and tightly regulated within GBM cells (Kou et al. 2022). This warrants analysis of changes that occur following ectopic RYBP expression. This could be measured using a free fatty acid assay. RYBP expression could possibly lead to an increase in free fatty acid if it interrupts the mechanisms required to store said fatty acid which could in turn cause cytotoxicity and confer a tumor suppressive

role. Alternatively, ectopic RYBP expression could lead to a decrease in free fatty acid if its expression inhibits fatty acid synthesis, depleting the necessary requirements for the GBM cells to grow and proliferate, also demonstrating a tumor suppressive role.

Further, the molecular mechanisms through which RYBP exerts its anti-tumor effects in GBM cells, remain to be elucidated. For example, other changes in EMT marker levels upon RYBP expression would help reveal how RYBP antagonizes migration and invasion in GBM. Also, measuring EGFR levels could provide insight, as aberrant signaling can lead to enhanced EMT (Witsch et al. 2010; Tong et al. 2018). Investigations into other apoptotic markers would also help elucidate the way in which RYBP plays a tumor suppressive role as to assess its viability as a new gene-targeted therapy or to illuminate cellular pathways that RYBP participates in that could lead to the development of more effective, targeted therapies.

Overall, our work has elucidated a novel tumor suppressive role of RYBP in GBM. We found significant reductions in migration and invasion of U-118 and T98G GBM cells upon ectopic RYBP expression. What appeared to be a decrease in vimentin following RYBP expression supports the idea that RYBP can exert anti-tumor effects through changes to EMT machinery. An increase seemed to be seen in N-cadherin levels, contrary to the typical EMT program. However, increased N-cadherin in glioma led to reduced cell invasion, suggesting RYBP may be operating as a tumor suppressor through a contextually distinct EMT program in non-epithelial GBM cells. We also saw what appeared to be increased cleaved caspase-3 levels once RYBP was ectopically expressed in T98G cells, indicating it may also play a role in inducing GBM cell apoptosis. More work is needed to fully characterize the cellular and molecular mechanisms behind RYBP's tumor suppressive abilities to fully assess RYBP's potential for gene-targeted therapeutics, but our work has demonstrated an important and novel role of RYBP in tumor suppression in GBM.

References

Al-Aamri HM, Irving HR, Bradley C, Meehan-Andrews T. 2021. Intrinsic and extrinsic apoptosis responses in leukemia cells following daunorubicin treatment. *BMC Cancer*. 21:438.

Ali M, Strickfaden H, Lee BL, Spyracopoulos L, Hendzel MJ. 2018. RYBP is a K63-ubiquitin-chain-binding protein that inhibits homologous recombination repair. *Cell reports*. 22(2):383–395.

Arrigoni R, Alam SL, Wamstad JA, Bardwell VJ, Sundquist WI, Schreiber-Agus N. 2006. The Polycomb-associated protein Rybp is a ubiquitin binding protein. *FEBS Letters*. 580(26):6233–6241.

Asano K, Asano K, Duntsch CD, Zhou Q, Weimar JD, Bordelon D, Robertson JH, Pourmotabbed T. 2004. Correlation of N-cadherin expression in high grade gliomas with tissue evasion. *J Neuro-Onco*. 70:3-15.

Bracken AP, Brien GL, Verrijzer CP. 2019. Dangerous liaisons: interplay between SWI/SNF, NuRD, and Polycomb in chromatin regulation and cancer. *Genes Dev*. 33(15-16):936–959.

Camand E, Peglion F, Osmani N, Sanson M, Etienne-Manneville S. 2012. N-cadherin expression level modulates integrin-mediated polarity and strongly impacts on the speed and directionality of glial cell migration. *J Cell Sci*. 125(4):844-857.

Cao ZQ, Wang Z, Leng P. 2019. Aberrant N-cadherin expression in cancer. *Biomed Pharmacotherapy*. 118:109320.

Cao R, Tsukadam Y, Zhang Y. 2005. Role of Bmi-1 and Ring1A in H2A ubiquitylation and Hox gene silencing. *Mol Cell.* 20:845-854.

Cao R, Wang L, Wang W, Xia L, Erdjument-Bromage H, Tempst P, Jones RS, Zhang Y. 2002. Role of histone H3 lysine 27 methylation in Polycomb-group silencing. *Sci*. 298:1039-1043.

Chan HL, Morey L. 2019. Emerging roles for Polycomb-group proteins in stem cells and cancer. *Trends Biochem Sci*. 44(8):688–700.

Chen D, Zhang J, Li M, Rayburn ER, Wang H, Zhang R. 2009. RYBP stabilizes p53 by modulating MDM2. *EMBO Reports.* 10:2(166-172).

Dinglin K., Ding L, Li Q, Liu Y, Zhang J, Yao H. 2017. RYBP inhibits progression and metastasis of lung cancer by suppressing EGFR signaling and epithelial-mesenchymal transition. *Transl Onco*. 10(2):280-287.

Fernandes C, Costa A, Osório L, Lago RC, Linhares P, Carvalho B, Caeiro C. 2017. Current Standards of Care in Glioblastoma Therapy. In: De Vleeschouwer S, editor. Glioblastoma. Brisbane (AU): Codon Publications. 197-241.

Friedl P, Alexander S. 2011. Cancer invasion and the microenvironment: plasticity and reciprocity. *Cell*. 147(5):992-1009.

Fursova NA, Blackledge NP, Nakayama M, King HW, Koseki H, Klose RJ. 2019. Synergy between variant PRC1 complexes defines Polycomb-mediated gene repression. *Mol Cell.* 74:1020-1036.

Gao Z, Zhang J, Bonasio R, Strino F, Sawai A, Parisi F, Kluger Y, Reinberg D. 2012. PCGF homologs, CBX proteins, and RYBP define functionally distinct PRC1 family complexes. *Mol Cell.* 45:344-356.

Garcia E, Marcos-Gutierrez C, del Mar Lorente M, Moreno JC, Vidal M. 1999. RYBP, a new repressor protein that interacts with components of the mammalian Polycomb complexes, and with the transcription factor YY1. *EMBO J.* 12:3404-3418.

Gearhart MD, Corcoran CM, Wanstad JA, Bardwell VJ. 2006. Polycomb group and SCF ubiquitin ligases are found in a novel BCOR complex that is recruited to BCL6 targets. *Mol Cell Bio.* 26:(18):6880-6889.

Geng Z, Gao Z. 2020. Mammalian PRC1 complexes: compositional complexity and diverse molecular mechanisms. *Int J Mol Sci.* 21:8594.

Haldbo-Classen L, Amidi A, Wu LM, Lukacova S, Oettingen G, Lassen-Ramshad Y, Zachariae R, Kallehauge JF, Høyer M. 2021. Associations between patient-reported outcomes and radiation dose in patients treated with radiation therapy for primary brain tumours. *Clin and Transl Rad Onc.* 31:86-92.

Iwadate Y. 2016. Epithelial-mesenchymal transition in glioblastoma progression. *Oncol Lett*. 11(3):1615-1620.

Jin FE, Xie B, Xian HZ, Wang JH. 2021. Knockdown of miR-125b-5p inhibits the proliferation and invasion of gastric carcinoma cells by targeting RYBP. *Kaohsiung J Med Sci.* 37(10):863–871.

Ke Y, Guo W, Huang S, Li Y, Guo Y, Liu X, Jin Y, Ma H. 2020. RYBP inhibits esophageal squamous cell carcinoma proliferation through downregulating CDC6 and CDC45 in G1-S phase transition process. *Life Sciences*. 250:117578.

Kerr JF, Wyllie AH, Currie AR. 1972. Apoptosis: a basic biological phenomenon with wide-ranging implications in tissue kinetics. *Br J Cancer*. 26(4):239–257.

Kou Y, Geng F, Guo D. 2022. Lipid metabolism in glioblastoma: from de novo synthesis to storage. *Biomedicines*. 10(8):1943.

Kovacs G, Szabo V, Pirity MK. 2016. Absence of Rybp Compromises Neural Differentiation of Embryonic Stem Cells. *Stem Cells Int*. 2016:4034620.

Krohn A, Seidel A, Burkhardt L, Bachmann F, Mader M, Grupp K, Eichenauer T, Becker A, Adam M, Graefen M, Huland H, Kurtz S, Steurer S, Tsourlakis MC, Minner S, Michl U, Schlomm T, Sauter G, Simon R, Sirma H. 2013. Recurrent deletion of 3p13 targets multiple tumour suppressor genes and defines a distinct subgroup of aggressive ERG fusion-positive prostate cancers. *J Patho. 231*(1):130–141.

Kuzmichev A, Nishioka K, Erdjument-Bromage H, Tempst P, Reinberg D. 2002. Histone methyltransferase activity associated with a human multiprotein complex containing the Enhancer of Zeste protein. *Genes Dev*. 16(22):2893–2905.

Lando M, Wilting SM, Snipstad K, Clancy T, Bierkens M, Aarnes EK, Holden M, Stokke T, Sundfør K, Holm R, Kristensen GB, Steenbergen RD, Lyng H. 2013. Identification of eight candidate target genes of the recurrent 3p12-p14 loss in cervical cancer by integrative genomic profiling. *J Patho.* 230(1):59–69.

Lewis EB. 1978. A gene complex controlling segmentation in *Drosophila*. *Nature*. 276:565-570.

Li G, Warden C, Zou Z, Neman J, Krueger JS, Jain A, Jandial R, Chen M. 2013. Altered expression of Polycomb group genes in glioblastoma multiforme. *PloS one*. *8*(11):e80970.

Li M, Zhang S, Zhao W, Hou C, Ma X, Li X, Huang B, Chen H, Chen D. 2019. RYBP modulates stability and function of Ring1B through targeting UBE3A. *FASEB J*. *33*(1):683–695.

Liu CY, Lin HH, Tang MJ, Wang YK. 2015. Vimentin contributes to epithelial-mesenchymal transition cancer cell mechanics by mediating cytoskeletal organization and focal adhesion maturation. *Oncotarget*. 6(18):15966-15983.

Luan PB, Jia XZ, Yao J. 2020. MiR-769-5p functions as an oncogene by down-regulating RYBP expression in gastric cancer. *Euro Rev Med Pharmaco Sci*. 24(12):6699–6706.

Ma W, Zhang X, Li M, Ma X, Huang B, Chen H, Chen D. 2016. Proapoptotic RYBP interacts with FANK1 and induces tumor cell apoptosis through the AP-1 signaling pathway. *Cell Signal* 28:779-787.

Matthews J, Kuchling F, Baez-Nieto D, Diberardinis M, Pan JQ, Levin M. 2022. Ion Channel Drugs Suppress Cancer Phenotype in NG108-15 and U87 Cells: Toward Novel Electroceuticals for Glioblastoma. *Cancers.* 14(6):1499.

Maybee DV, Psaras AM, Brooks TA, Ali MAM. 2022. RYBP sensitizes cancer cells to PARP inhibitors by regulating ATM activity. *Int J Mol Sci.* 23(19):11764.

McKelvey KJ, Wilson EB, Short S, Melcher AA, Biggs M, Diakos CI, Howell VM. 2021. Glycolysis and fatty acid oxidation inhibition improves survival in glioblastoma. *Front Oncol.* 11:633210.

Neira JL, Jiménez-Alesanco A, Rizzuti B, Velazquez-Campoy A. 2021. The nuclear localization sequence of the epigenetic factor RYBP binds to human importin α3. *Biochim Biophys Acta Proteins Proteom*. 1869(8):140670.

Novikov NM, Zolotaryova SY, Gautreau AM, Denisov EV. 2021. Mutational drivers of cancer cell migration and invasion. *Br J Cancer*. 124:102-114.

O'Brien J, Hayder H, Zayed Y, Peng C. 2018. Overview of microRNA biogenesis, mechanisms of actions, and circulation. *Front Endocrin.* 9:402.

Ohgaki H and Kleihues P. 2013. The Definition of Primary and Secondary Glioblastoma. *Clin Cancer Research.* 19(4):764-772

Ostram QT, Cioffi G, Waite K, Kruchko C, Barnholtz-Sloan JS. 2021. CBTRUS Statistical Report: Primary Brain and Other Central Nervous System Tumors Diagnosed in the United States in 2014–2018. *Neuro-Oncology.* 23:iii1-iii105.

Paro R. 1990. Imprinting a determined state into the chromatin of *Drosophila*. *Elsevier Sci. Pub. Ltd.* 6:12.

Porter AG, Jänicke RU. 1999. Emerging roles of caspase-3 in apoptosis. *Cell Death and Differentiation*. 6:99-104.

Ricciardi M, Zanotto M, Malpeli G, Bassi G, Perbellini O, Chilosi M, Bifari F, Krampera M. 2015. Epithelial-to-mesenchymal transition (EMT) induced by inflammatory priming elicits mesenchymal stromal cell-like immune-modulatory properties in cancer cells. *Br J Cancer.* 112:1067–1075.

Rose NR, King HW, Blackledge NP, Fursova N, Ember KJI, Fisher R, Kessler BM, Klose RJ. 2016. RYBP stimulates PRC1 to shape chromatin-based communication between Polycomb repressive complexes. *eLIFE*. 5:e18591.

Sánchez-Beato M, Sánchez E, González-Carreró J, Morente M, Díez A, Sánchez-Verde L, Martín MC, Cigudosa JC, Vidal M, Piris MA. 2006. Variability in the expression of Polycomb proteins in different normal and tumoral tissues. A pilot study using tissue microarrays. *Mod Pathol.* 19(5):684–694.

Sari C, Kolayli S, Eyupoglu FC. 2021. A Comparative Study of MTT and WST-1 Assays in Cytotoxicity Analysis. *Haydar Num Med J.* 61(3):281-288.

Sasaki D, Imaizumi Y, Hasegawa H, Osaka A, Tsukasaki K, Choi YL, Mano H, Marquez VE, Hayashi T, Yanagihara K, Moriwaki Y, Miyazaki Y, Kamihira S, Yamada Y. 2011. Overexpression of Enhancer of zeste homolog 2 with trimethylation of lysine 27 on histone H3 in adult T-cell leukemia/lymphoma as a target for epigenetic therapy. *Haematologica*. 96(5):712–719.

Sawa C, Yoshikawa T, Matsuda-Suzuki F, Deléhouzée S, Goto M, Watanabe H, Sawada JI, Kataoka K, Handa H. 2002. YEAF1/RYBP and YAF-2 are functionally distinct members of a cofactor family for the YY1 and E4TF1/hGABP transcription factors. *J Bio Chem*. 277(25):22484-22490.

Skidmore CJ, Daview MI, Goodwin PM, Halldorsson H, Lewis PJ, Shall S, Zia'ee A. 1979. The involvement of poly(ADP-ribose) polymerase in the degradation of NAD caused by y-radiation and N-methyl-N-nitrosourea. *Eur J Biochem*. 101:135-142.

Sun M, Huang N, Tao Y, Wen R, Zhao G, Zhang X, Xie Z, Cheng Y, Mao J, Liu G. 2022. The efficacy of temozolomide combined with levetiracetam for glioblastoma (GBM) after surgery: a study protocol for a double-blinded and randomized controlled trial. *Trials*. 23:234.

Sung H, Ferlay J, Siegel RL, Laversanne M, Soerjomataram I, Jemal A, Bray F. 2021. Global cancer statistics 2020: GLOBOCAN estimates of incidence and mortality worldwide for 36 cancers in 185 countries. *CA: A Cancer J for Clin.* 71(3):209-249.

Sutus E, Henry S, Adorján L, Kovács G, Pirity MK. 2022. RYBP regulates Pax6 during in vitro neural differentiation of mouse embryonic stem cells. *Sci Rep*. 12(1):2364.

Tamburri S, Lavarone E, Fernandez-Perez D, Conway E, Zanotti M, Manganaro D, Pasini D. 2020. Histone H2AK119 mono-ubiquitination is essential for Polycomb-mediated transcriptional repression. *Mol Cell.* 77:840-856.

Tan K, Zhang X, Cong X, Huang B, Chen H, Chen D. 2017. Tumor suppressor RYBP harbors three nuclear localization signals and its cytoplasm-located mutant exerts more potent anti-cancer activities than corresponding wild type. *Cell Sig.* 29:127-137.

Tong AH, Tan J, Zhang JH, Xu FJ, Li FY. 2019. Overexpression of RYBP inhibits proliferation, invasion, and chemoresistance to cisplatin in anaplastic thyroid cancer cells via the EGFR pathway. *J. Biochem Mol. Tox*. 33(2):e22241.

Wang W, Qin JJ, Voruganti S, Nag S, Zhou J, Zhang R. 2015. Polycomb group (PcG) proteins and human cancers: multifaceted functions and therapeutic implications. *Med Res Rev.* 35(6):1220-1267.

Warburg O. 1925. The metabolism of carcinoma cells. *J Cancer Res*. 9(1):148-163.

Wei C, Jia L, Huang X, Tan J, Wang M, Niu J, Hou Y, Sun J, Zeng P, Wang J, Qing L, Ma L, Liu X, Tang X, Li F, Jiang S, Liu J, Li T, Fan L, Sun Y, Gao J, Li C, Ding J. 2022. CTCF organizes inter-A compartment interactions through RYBP-dependent phase separation. *Cell Res*. 32(8):744-760.

Witsch E, Sela M, Yarden Y. 2010. Roles for growth factors in cancer progression. *Physiology (Bethesda)*. 25(2):85-101.

Wong RS. 2011. Apoptosis in cancer: from pathogenesis to treatment. *J Exp Clin Cancer Res.* 30(87).

Xian Y, Wang L, Yao B, Yang W, Mo H, Zhang L, Tu K. 2019. MicroRNA-769-5p contributes to the proliferation, migration and invasion of hepatocellular carcinoma cells by attenuating RYBP. *Biomed Pharmaco.* 118:109343.

Zhao J, Wang M, Chang L, Yu J, Song A, Liu C, Huang W, Zhang T, Wu X, Shen X, Zhu B, Li G. 2020. RYBP/YAF2-PRC1 complexes and histone H1-dependent chromatin compaction mediate propagation of H2AK119ub1 during cell division. *Nat Cell Biol.* 22(4):439–452.

Zhao W, Zhang S, Wang X, Ma X, Huang B, Chen H, Chen D. 2019. ETS1 targets RYBP transcription to inhibit tumor cell proliferation. *Biochem Biophys Res Com*. 509(3):810–816.

Zheng L, Schickling O, Peter ME, Lenardo MJ. 2001. The Death Effector Domain-associated Factor Plays Distinct Regulatory Roles in the Nucleus and Cytoplasm. *J. Bio. Chem.* 276:34(31945-31952).

Zhou H, Li J, Zhang Z, Ye R, Shao N, Cheang T, Wang S. 2016. RING1 and YY1 binding protein suppresses breast cancer growth and metastasis. *Int J of Onco. 49*(6):2442–2452.